J. Appl. Math. & Informatics Vol. **39***(2021), No. 5 - 6, pp. 655 - 676*
https://doi.org/10.14317/jami.2021.655

UNIFORMLY CONVERGENT NUMERICAL SCHEME FOR A SINGULARLY PERTURBED DIFFERENTIAL-DIFFERENCE EQUATIONS ARISING IN COMPUTATIONAL NEUROSCIENCE

IMIRU TAKELE DABA AND GEMECHIS FILE DURESSA*

Abstract. A parameter uniform numerical scheme is proposed for solving singularly perturbed parabolic partial differential-difference convection-diffusion equations with a small delay and advance parameters in reaction terms and spatial variable. Taylor's series expansion is applied to approximate problems with the delay and advance terms. The resulting singularly perturbed parabolic convection-diffusion equation is solved by utilizing the implicit Euler method for the temporal discretization and finite difference method for the spatial discretization on a uniform mesh. The proposed numerical scheme is shown to be an $\varepsilon-$uniformly convergent accurate of the first order in time and second-order in space directions. The efficiency of the scheme is proved by some numerical experiments and by comparing the results with other results. It has been found that the proposed numerical scheme gives a more accurate approximate solution than some available numerical methods in the literature.

AMS Mathematics Subject Classification : 35B25, 65M06, 65N12.
Key words and phrases : Finite difference method, implicit Euler method, differential-difference equations, singular perturbation problem.

1. Introduction

A differential-difference equation with at least one delay parameter in which the highest order derivative is multiplied by an arbitrary small parameter ε, termed as singular perturbation parameter, is called the singularly perturbed differential-difference equation (SPDDE). Such types of SPDDEs have a variety of applications in modeling the neuronal variability [1], in the study of bistable devices [2] and evolutionary biology [3], to describe the human pupil-light reflex [4], in the study of variational problems of control theory [5]. In 1991, Musila

Received August 15, 2020. Revised May 1, 2021. Accepted May 4, 2021. *Corresponding author.

and Lansky [7] gave generalization for Stein's model [1] and proposed a model to treat the time evolution trajectories of the membrane potential in terms of singularly perturbed delay parabolic partial differential equations (SPDPPDEs) as:

$$\frac{\partial u}{\partial t}+\frac{\sigma^2}{2}\frac{\partial^2 u}{\partial x^2}+\left(\mu_D-\frac{x}{\tau}\right)\frac{\partial u}{\partial x}+\lambda_s u(x+a_s,t)+\omega_s u(x+i_s,t)-(\lambda_s+\omega_s)u(x,t)=0, \tag{1}$$

where σ and μ_D are diffusion moments of Wiener process characterizing the influence of dendritic synapses on the cell excitability. The membrane potential decays exponentially to the resting level with a membrane time constant τ . The first derivative term is obtained because of the exponential decay between two consecutive jumps caused by the input processes. The reaction terms correspond to the superposition of excitatory and inhibitory inputs, and we can assume that they are Poissonian [7]. This model makes available time evolution of the trajectories of the membrane potential. The excitatory input contributes to the membrane potential by an amplitude a_s with intensity λ_s and similarly, the inhibitory input contributes by an amplitude i_s with intensity ω_s. The solution of model 1 with small values of singular perturbation parameter ε exhibits boundary layer(s). Due to the presence of the boundary layer(s) in the solution, one can hardly derive any analytical solutions for Eq. 1. Hence, to stimulate model 1, one has to look for suitable numerical methods.

In [8, 9, 6, 12, 13, 14, 10, 11, 15], authors developed different numerical methods to solve a class of SPDPPDEs and discussed the effect of shifts on the boundary layer behaviour of the solutions using adaptive mesh, fitted operator, and method of line. In [6, 8, 9, 12, 13, 14, 15], authors restricted their study to the case when the shift arguments are less than the singular perturbation parameter and used Taylor's series expansion to approximate the shift arguments. In [[10],[11], authors constructed a numerical scheme that works in both cases, i.e., small and bigger shift arguments. Nevertheless, the former method is not a parameter uniform. However, the development of the solution methodologies to solve SPDPPDEs with small and general shift arguments for the past decade is still at the infant stage. This motivates the authors to construct a parameter uniform numerical scheme for SPDPPDEs.

In this paper, we proposed an $\varepsilon-$ uniform numerical method for solving a second-order SPDPPDE with delay and advance parameters in the reaction terms and the space variable using the implicit Euler scheme to discretize the time variable and finite difference method to discretize the spatial variable on a uniform step size. The novelty of the presented method lies in the fact that it does not depends on a specially designed mesh

The rest of this paper is organized as follows: Section 2 is devoted to the formulation of the problem and properties of the solution of the continuous problem. The construction of the numerical scheme is briefly described in Section 3. Error estimates for the proposed method are presented in Section 4. In Section 5, numerical examples and results are given to confirm the theoretical

investigations. Finally, the conclusion of this study is given in Section 6
Notations: Throughout this paper, N and M denote the number of mesh points in x and t directions respectively. C denotes a generic positive constant independent of the singular perturbation parameter ε and the mesh sizes.

2. Problem Formulation

We consider a class of second-order singularly perturbed parabolic partial differential-difference equations with small mixed shift arguments in the spatial variable and reaction terms on the rectangular domain $D = \Omega_x \times \Omega_t = (0,1) \times (0,T]$ for fixed positive number T:

$$\begin{cases} \frac{\partial u(x,t)}{\partial t} - \varepsilon^2 \frac{\partial^2 u(x,t)}{\partial x^2} + a(x)\frac{\partial u(x,t)}{\partial x} + b(x)u(x-\delta,t) + c(x)u(x,t) \\ +d(x)u(x+\eta,t) = f(x,t)(x,t) \in D, \\ u(x,0) = u_0(x), x \in D_0 = \{(x,0) : x \in \overline{\Omega}_x\}, \\ u(x,t) = \phi(x,t), \forall (x,t) \in D_L = \{(x,t) : -\delta \le x \le 0, t \in (0,T]\}, \\ u(x,t) = \psi(x,t), \forall (x,t) \in D_R = \{(x,t) : 1 \le x \le 1+\eta, t \in (0,T]\}, \end{cases} \tag{2}$$

where ε is a small perturbation parameter $0 < \varepsilon \ll 1$, delay parameter δ and advance parameter η are assumed to be of order $o(\varepsilon)$. The functions $a(x)$, $b(x)$, $c(x)$, $d(x)$, $f(x,t)$, $\phi(x,t)$, $\psi(x,t)$ and $u_0(x)$ are assumed to be sufficiently smooth, bounded and independent of ε . It is also assumed that

$$b(x) + c(x) + d(x) \ge q^* > 0, \ \forall x \in \overline{\Omega}_x \tag{3}$$

for some positive constant q^*. When the delay and advance parameter is zero (i.e., $\delta, \eta = 0$), the above equation reduces to a standard singularly perturbed parabolic convection-diffusion problem which is with small singular perturbation parameter ε and exhibits layer(s) depending on the sign of $a(x)$. If $a(x) > 0$, then a boundary layer appears in the neighborhood of $x = 1$. If $a(x) < 0$, then a boundary layer appears in the neighborhood of $x = 0$. The interior layer may occur in the case of a turning point, that is where $a(x)$ changes the sign in $\overline{\Omega}_x$. However, the layer is maintained for sufficiently small shifts $\delta, \eta \neq 0$.

2.1. Estimates for the delay and advance parameters. When the shift parameters δ and η are smaller than singular perturbation parameter ε, the use of Taylor's series expansion for the terms containing shift arguments is valid [19]. In this paper, we considered the case when $\delta, \eta < \varepsilon$. Thus, to approximate the terms with delay and advance parameters, we apply Taylor's series expansion as follows:

$$u(x-\delta,t) = u(x,t) - \delta\frac{\partial u(x,t)}{\partial x} + O(\delta^2), \tag{4}$$

$$u(x+\eta,t) = u(x,t) + \eta\frac{\partial u(x,t)}{\partial x} + O(\eta^2). \tag{5}$$

Now substituting Eq.(4) and Eq. (5) into Eq. (2), we obtain:

$$\begin{cases} \frac{\partial u(x,t)}{\partial t} - \varepsilon^2 \frac{\partial^2 u(x,t)}{\partial x^2} + p(x)\frac{\partial u(x,t)}{\partial x} + q(x)u(x,t) = f(x,t), \\ u(x,0) = u_0(x), x \in \overline{\Omega}_x, \\ u(0,t) = \phi(0,t), t \in \overline{\Omega}_t, \\ u(1,t) = \psi(1,t), t \in \overline{\Omega}_t, \end{cases} \tag{6}$$

where, $p(x) = a(x) - \delta b(x) + \eta d(x),\ q(x) = b(x) + c(x) + d(x)$.
Since $p(x) \geq \alpha > 0$ and $q(x) \geq q^* > 0$ for some constants α and q^* the solution of Eq.(6) exhibits an exponential boundary layer at $x = 1$. For small δ and η, Eq.(2) and Eq.(6) are asymptotically equivalent, because the difference between the two equations is the order of $O(\delta^2, \eta^2)$.

To avoid the presence of a singularity in the numerical solution it is required that the given data $u_0(x), \phi(x,t)$ and $\psi(x,t)$ satisfy certain compatibility conditions at the corner points of the given domain. The required compatibility conditions are as follows [16]:

$$\begin{cases} u_0(0) = \phi(0,0), \\ u_0(1) = \psi(1,0) \end{cases} \tag{7}$$

and

$$\begin{cases} \frac{\partial \phi(0,0)}{\partial t} - \varepsilon^2 \frac{\partial^2 u_0(0)}{\partial x^2} + p(0)\frac{\partial u_0(0)}{\partial x} + q(0)u_0(0) = f(0,0), \\ \frac{\partial \psi(1,0)}{\partial t} - \varepsilon^2 \frac{\partial^2 u_0(1)}{\partial x^2} + p(1)\frac{\partial u_0(1)}{\partial x} + q(1)u_0(1) = f(1,0). \end{cases} \tag{8}$$

From the compatibility conditions (7) and (8) , we have,

$$|u(x,t) - u(x,0)| = |u(x,t) - u_0(x)| \leq Ct,\ \forall (x,t) \in \overline{D}, \tag{9}$$

$$|u(x,t) - u(0,t)| = |u(x,t) - \phi(0,t)| \leq C(1-x),\ \forall (x,t) \in \overline{D}. \tag{10}$$

For the proof of Eqs. (9) and (10) one can refer [13]

Remark 2.1. We note that there does not exist a constant C independent of ε such that

$$|u(x,t) - u(1,t)| = |u(x,t) - \psi(1,t)| \leq Cx,\ \forall\, (x,t) \in \overline{D}$$

because a boundary layer occurs near $x = 1$.

2.2. Properties of the solution of the continuous problem.

Lemma 2.1. *The solution $u(x,t)$ of the continuous problem* (6) *is bounded by*

$$|u(x,t)| \leq C,\ \forall (x,t) \in \overline{D}.$$

Proof. From the triangular inequality and Eq. (9), we have

$$|u(x,t)| = |u(x,t) - u(x,0) + u(x,0)| \leq |u(x,t) - u_0(x)| + |u_0(x)| \leq Ct + |u_0(x)|\,.$$

Since $t \in (0,T]$, so it is bounded and $u_0(x) \in C^{2,1}(\overline{D})$. Therefore, $Ct + |u_0(x)|$ is bounded by some generic positive constant C and we get

$$|u(x,t)| \leq C, \ \forall (x,t) \in \overline{D}.$$

□

The differential operator $L_\varepsilon = \frac{\partial}{\partial t} - \varepsilon^2 \frac{\partial^2}{\partial x^2} + p(x)\frac{\partial}{\partial x} + q(x)$ in Eq.(6) satisfies the following maximum principle.

Lemma 2.2. *(Continuous Maximum Principle). Let $\Phi(x,t) \in C^{2,1}\overline{D}$. If $\Phi(x,t) \geq 0, \forall (x,t) \in \partial D$ and $L_\varepsilon \Phi(x,t) \geq 0, \forall (x,t) \in D$, then $\Phi(x,t) \geq 0, \forall (x,t) \in \overline{D}$.*

Proof. Let $(x^*,t^*) \in \overline{D}$ be such that

$$\Phi(x^*,t^*) = \min_{(x,t)\in\overline{D}} \Phi(x,t),$$

and suppose that $\Phi(x^*,t^*) < 0$, then we have $(x^*,t^*) \notin \partial D$. Also we have $\Phi_x(x^*,t^*) = 0, \Phi_t(x^*,t^*) = 0$ and $\Phi_{xx}(x^*,t^*) \geq 0$. Then

$$L_\varepsilon \Phi(x^*,t^*) = \frac{\partial \Phi(x^*,t^*)}{\partial t} - \varepsilon^2 \frac{\partial^2 \Phi(x^*,t^*)}{\partial x^2} + p(x)\frac{\partial \Phi(x^*,t^*)}{\partial x} + q(x)\Phi(x^*,t^*) < 0,$$

which contradict to the assumption made above. It follows that $\Phi(x^*,t^*) \geq 0$ and hence $\Phi(x,t) \geq 0, \forall (x,t) \in \overline{D}$. □

Lemma 2.3. *(Continuous stability estimate). Let $u(x,t)$ be the solution of the problem* (6)*, then we have*

$$\|u\| \leq (q^*)^{-1} \|f\| + \max\left\{|u_0(x)|, \max\left\{|\phi(x,t)|, |\psi(x,t)|\right\}\right\},$$

where, $\|.\|$ is the L_∞ norm given by $\|u\| = \max_{(x,t)\in\overline{D}} |u(x,t)|$.

Proof. Let $\Phi^{\pm}(x,t)$ be two barrier functions defined by

$$\Phi^{\pm}(x,t) = (q^*)^{-1} \|f\| + \max\left\{|u_0(x)|, \max\left\{|\phi(x,t)|, |\psi(x,t)|\right\}\right\} \pm u(x,t).$$

Then at the initial value

$$\Phi^{\pm}(x,0) = (q^*)^{-1} \|f\| + \max\left\{|u_0(x)|, \max\left\{|\phi(x,0)|, |\psi(x,0)|\right\}\right\} \pm u(x,0) \geq 0.$$

At the two end points

$$\Phi^{\pm}(0,t) = (q^*)^{-1} \|f\| + \max\left\{|u_0(0)|, \max\left\{|\phi(0,t)|, |\psi(0,t)|\right\}\right\} \pm u(0,t) \geq 0,$$

$$\Phi^{\pm}(1,t) = (q^*)^{-1} \|f\| + \max\left\{|u_0(1)|, \max\left\{|\phi(1,t)|, |\psi(1,t)|\right\}\right\} \pm u(1,t) \geq 0.$$

and

$$\begin{aligned}
&L_\varepsilon \Phi^{\pm}(x,t) = \tfrac{\partial \Phi^{\pm}(x,t)}{\partial t} - \varepsilon^2 \tfrac{\partial^2 \Phi^{\pm}(x,t)}{\partial x^2} + p(x)\tfrac{\partial \Phi^{\pm}(x,t)}{\partial x} + q(x)\Phi^{\pm}(x,t) \\
&= q(x)\left((q^*)^{-1} \|f\| + \max\left\{|u_0(x)|, \max\left\{|\phi(x,t)|, |\psi(x,t)|\right\}\right\}\right) \pm L_\varepsilon u(x,t) \\
&= q(x)\left((q^*)^{-1} \|f\| + \max\left\{|u_0(x)|, \max\left\{|\phi(1,t)|, |\psi(x,t)|\right\}\right\}\right) \pm f(x,t) \\
&\geq q^*\left(\max\left\{|u_0(x)|, \max\left\{|\phi(x,t)|, |\psi(x,t)|\right\}\right\}\right) + \|f\| \pm f(x,t) \\
&\geq 0, \text{ since } q^* > 0, \text{and } \|f\| \geq f(x,t).
\end{aligned}$$

This implies that $L_\varepsilon \Phi^{\pm}(x,t) \geq 0$. Hence by Lemma (2.2) we have, $\Phi^{\pm}(x,t) \geq 0 \; \forall (x,t) \in \overline{D}$, which gives

$$\|u\| \leq (q^*)^{-1} \|f\| + \max\left\{|u_0(x)|, \max\left\{|\phi(x,t)|, |\psi(x,t)|\right\}\right\}$$

the proof is completed. □

Lemma 2.4. *The bound on the derivative of the solution $u(x,t)$ of the problem in (6) with respect to x is given by*

$$\left|\frac{\partial^i u(x,t)}{\partial x^i}\right| \leq C\left(1 + (\varepsilon^2)^{-i} \exp\left(\frac{-(p^*(1-x))}{\varepsilon^2}\right)\right), (x,t) \in \overline{D}, 0 \leq i \leq 4.$$

Proof. The details proof of the lemma is given in [18]. □

3. Construction of the Numerical Scheme

3.1. Temporal Discretization. In this section, we discretize Eq. (6) by utilizing the implicit Euler method on a uniform mesh Δt is defined by:

$$\Omega_t^M = \{t_i = t_0 + i\Delta t, \; i = 1, 2, ..., M, \; t_0 = 0, \Delta t = T/M\},$$

we obtain a system of ODEs:

$$\begin{cases} -\varepsilon^2 U_{xx}(x, t_{j+1}) + p(x)U_x(x, t_{j+1}) + Q(x)U(x, t_{j+1}) = g(x, t_{j+1}), \\ u(x,0) = u_0(x), x \in \overline{\Omega}_x, \\ u(0, t_{j+1}) = \phi(0, t_{j+1}), t \in \overline{\Omega}_t, \\ u(1, t_{j+1}) = \psi(1, t_{j+1}), t \in \overline{\Omega}_t, \end{cases} \tag{11}$$

where,

$$Q(x) = \left(q(x) + \frac{1}{\Delta t}\right), g(x, t_{j+1}) = \left(f(x, t_{j+1}) + \frac{U(x, t_j)}{\Delta t}\right).$$

The following lemmas show the consistency and stability of the solution of Eq. (11).

Lemma 3.1. *(Semi-discrete Maximum Principle). Let $\Phi(x, t_{j+1}) \in C^2\overline{\Omega}_x$. If $\Phi(0, t_{j+1}) \geq 0$, $\Phi(1, t_{j+1}) \geq 0$, and $L_\varepsilon \Phi(x, t_{j+1}) \geq 0, \forall x \in \Omega_x$, then $\Phi(x, t_{j+1}) \geq 0$, $\forall (x) \in \overline{\Omega}_x$.*

Proof. Let $(x^*, t_{j+1}) \in \left\{(x, t_{j+1}) : x \in \overline{\Omega}_x\right\}$ be such that

$$\Phi(x^*, t_{j+1}) = \min_{x \in \overline{\Omega}_x} \Phi(x, t_{j+1}),$$

and suppose that $\Phi(x^*, t_{j+1}) < 0$, then we have $(x^*, t_{j+1}) \notin \{(0, t_{j+1}), (1, t_{j+1})\}$. Also we have $\Phi_x(x^*, t_{j+1}) = 0$, and $\Phi_{xx}(x^*, t_{j+1}) \geq 0$. Then

$$L_\varepsilon \Phi(x^*, t_{j+1}) = -\varepsilon^2 \Phi_{xx}(x^*, t_{j+1}) + p(x)\Phi_x(x^*, t_{j+1}) + Q(x)\Phi(x^*, t_{j+1}) < 0,$$

which is contradict to our assumption. It follows that $\Phi(x^*, t_{j+1}) \geq 0$ and hence $\Phi(x, t_{j+1}) \geq 0, \forall x \in \overline{\Omega}_x$. □

Lemma 3.2. *Suppose* $\left|\frac{\partial^k u(x,t)}{\partial x^k}\right| \leq C,\ \forall\,(x,t) \in \overline{D}, k = 0, 1, 2$. *Then the local error estimate in the temporal direction is given by*

$$\|e_{j+1}\| \leq C\,(\Delta t)^2,$$

where $e_{j+1} = u(x, t_{j+1}) - U(x, t_{j+1})$ *is the local error estimate in the temporal direction at* j^{th} *time level.*

Proof. Since the function $U(x, t_{j+1})$ satisfies

$$L_\varepsilon^M U(x, t_{j+1}) = g(x, t_{j+1}) \tag{12}$$

and the solution of the continuous problem (2) is smooth enough, we have

$$\begin{aligned} g(x, t_{j+1}) &= L_\varepsilon^M u(x, t_{j+1}) + \int_{t_j}^{t_{j+1}} (t_j - \xi)\, \tfrac{\partial^2 u}{\partial t^2}\,(\xi)\, d\xi \\ &= L_\varepsilon^M u(x, t_{j+1}) + O\left((\Delta t)^2\right). \end{aligned} \tag{13}$$

From Eqs. (12) and (13), the local truncation error corresponding to (11) is given by $e_{j+1} = u(x, t_{j+1}) - U(x, t_{j+1})$ and satisfy the following boundary value problem:

$$\begin{aligned} L_\varepsilon^M e_{j+1} &= O\left((\Delta t)^2\right), \\ e_{j+1} &= \left(L_\varepsilon^M\right)^{-1} O\left((\Delta t)^2\right), \\ e_{j+1}(0) &= e_{j+1}(1) = 0. \end{aligned} \tag{14}$$

An application of maximum principle on the above operator L_ε^M gives

$$\|e_{j+1}\| \leq C\,(\Delta t)^2$$

the proof is completed. □

Lemma 3.3. *Under the hypothesis of the Lemma 3.2 global error estimate in the temporal direction is given by*

$$\|E_j\|_\infty \leq C(\Delta t),\ \forall\ j \leq T/\Delta t,$$

where E_j *is the global error estimate in the temporal direction at* $(j)th$ *time level.*

Proof. Using local error estimates up to jth time step given in Lemma 3.2, we get the following global error estimates at $(j+1)th$ time step

$$\begin{aligned} &\|E_j\|_\infty = \left\|\textstyle\sum_{i=1}^{j} e_i\right\|_\infty,\ j \leq T/\Delta t \\ &\leq \|e_1\|_\infty + \|e_2\|_\infty + \|e_3\|_\infty + \cdots + \|e_j\|_\infty \\ &\leq c_1 j\,(\Delta t)^2 \ \text{ by Lemma 3.2} \\ &\leq c_1\,(j\Delta t)\,\Delta t \\ &\leq c_1 T\,(\Delta t)\ \ (j\Delta t \leq T) \\ &\leq C\,(\Delta t), \end{aligned}$$

where C is a positive constant independent of ε and Δt. Therefore, the time semi-discretization process is uniformly convergent of first order. □

3.2. Spatial Discretization. In this section, we use the finite difference method for the spatial discretization of the problem (11) with a uniform step size, which can be written in the form of (denoting $U^{''}(x) = U_{xx}^{j+1}(x), U^{'}(x) = U_{x}^{j+1}(x), U(x) = U^{j+1}(x)$ and $g(x) = g(x, t_{j+1})$ for $0 \leq j \leq M$) :

$$-\varepsilon^2 U^{''}(x) + p(x)U^{'}(x) + Q(x)U(x) = g(x),\ 0 \leq x \leq 1, \tag{15}$$

subject to the boundary conditions

$$U(0) = \phi(0),\ U(1) = \psi. \tag{16}$$

For problems with a layer at the right end of the interval, from the theory of singular perturbations, it is known that the solution of Eqs. (15) and (16) is of the form [17] (page 22-26):

$$U(x) \approx U_0(x) + \frac{p(1)}{p(x)}\left(\psi - U_0(x)\right)\exp\left(-p(x)\frac{1-x}{\varepsilon^2}\right) + O(\varepsilon), \tag{17}$$

where $U_0(x)$ is the solution of reduced problem

$$p(x)U_0^{'}(x) + Q(x)U_0(x) = g(x),\ with,\ U_0(1) = \psi(1).$$

By taking the Taylor's series expansion for $p(x)$ about the point $'1'$ and restricting to their first terms, Eq. (17) becomes

$$U(x) \approx U_0(x) + \left(\psi - U_0(1)\right)\exp\left(-p(1)\left(\frac{1-x}{\varepsilon^2}\right)\right) + O(\varepsilon). \tag{18}$$

Now we divide the interval $[0, 1]$ into N equal parts with $h = 1/N$. Let $0 = x_0, x_1, x_2, \cdots, x_N = 1$ be the mesh points. Then, we have $x_i = ih,\ i = 0, 1, 2, \cdots, N$. By considering Eq. (18) at $x_i = ih$ as $h \to 0$, we obtain

$$\lim_{h\to 0} U(ih) \approx U_0(0) + \left(\psi - U_0(1)\right)\exp\left(-p(1)\left(\frac{1}{\varepsilon^2} - i\rho\right)\right) + O(\varepsilon), \tag{19}$$

where $\rho = \frac{h}{\varepsilon^2}$.
Let $U(x)$ be smooth function in the interval $[0, 1]$. Then by applying Taylor's series expansion, we have:

$$\begin{aligned} U(x_{i+1}) \approx U_{i+1} \approx U_i + hU_i^{'} + \frac{h^2}{2!}U_i^{''} + \frac{h^3}{3!}U_i^{(3)} + \frac{h^4}{4!}U_i^{(4)} + \frac{h^5}{5!}U_i^{(5)} + \frac{h^6}{2!}U_i^{(6)} \\ + \frac{h^7}{7!}U_i^{(7)} + \frac{h^8}{8!}U_i^{(8)} + O(h^9), \end{aligned} \tag{20}$$

and

$$\begin{aligned} U(x_{i-1}) \approx U_{i-1} \approx U_i - hU_i^{'} + \frac{h^2}{2!}U_i^{''} - \frac{h^3}{3!}U_i^{(3)} + \frac{h^4}{4!}U_i^{(4)} - \frac{h^5}{5!}U_i^{(5)} + \frac{h^6}{2!}U_i^{(6)} \\ - \frac{h^7}{7!}U_i^{(7)} + \frac{h^8}{8!}U_i^{(8)} - O(h^9). \end{aligned} \tag{21}$$

Adding Eq. (20) and Eq. (21), we get

$$U_{i-1} - 2U_i + U_{i+1} = \frac{2h^2}{2!}U_i^{''} + \frac{2h^4}{4!}U_i^{(4)} + \frac{2h^6}{2!}U_i^{(6)} + \frac{2h^8}{8!}U_i^{(8)} + O(h^{10}), \quad (22)$$

and the relation

$$U_{i-1}^{''} - 2U_i^{''} + U_{i+1}^{''} = \frac{2h^2}{2!}U_i^{(4)} + \frac{2h^4}{4!}U_i^{(6)} + \frac{2h^6}{6!}U_i^{(8)} + \frac{2h^8}{8!}U_i^{(10)} + O(h^{12}).$$

Substituting $\frac{h^4}{12}U_i^{(6)}$ from the above Eq. in (22), we obtain

$$U_{i-1} - 2U_i + U_{i+1} = \frac{h^2}{30}\left(U_{i-1}^{''} + 28U_i^{''} + U_{i+1}^{''}\right) + R, \quad (23)$$

where, $R = \frac{h^4}{20}U_i^{(4)} - \frac{13h^6}{302400}U_i^{(8)} + O(h^{(10)})$
Now from Eq. (15), we have

$$\varepsilon^2 U_{i+1}^{''} = p_{i+1}U_{i+1}^{'} + Q_{i+1}U_{i+1} - g_{i+1}, \quad (24)$$

$$\varepsilon^2 U_i^{''} = p_i U_i^{'} + Q_i U_i - g_i, \quad (25)$$

and

$$\varepsilon^2 U_{i-1}^{''} = p_{i-1}U_{i-1}^{'} + Q_{i-1}U_{i-1} - g_{i-1} \quad (26)$$

where we approximate $U_{i+1}^{'}, U_i^{'}$ and $U_{i-1}^{'}$ using non symmetric finite differences

$$U_i^{'} \approx \frac{U_{i+1} - U_{i-1}}{2h} + O\left(h^2\right), \quad (27)$$

$$U_{i+1}^{'} \approx \frac{3U_{i+1} - 4U_i + U_{i-1}}{2h} - hU_i^{"} + O\left(h^2\right), \quad (28)$$

and

$$U_{i-1}^{'} \approx \frac{-U_{i+1} + 4U_i - 3U_{i-1}}{2h} + hU_i^{"} + O\left(h^2\right). \quad (29)$$

Substituting Eqs. (27), (28) and (29) in Eqs. (25), (24) and (29) respectively and simplifying the Eq. (23), we get

$$\begin{aligned}
&\left(\varepsilon^2 + \tfrac{p_{i+1}h}{30} - \tfrac{p_{i-1}h}{30}\right)\left(\tfrac{U_{i-1}-2U_i+U_{i+1}}{h^2}\right) \\
&= \left(\tfrac{-p_{i-1}}{20h} + \tfrac{Q_{i-1}}{30} - \tfrac{7p_i}{15h} + \tfrac{p_{i+1}}{60h}\right)U_{i-1} + \left(\tfrac{p_{i-1}}{15h} + \tfrac{14Q_i}{15} - \tfrac{p_{i+1}}{15h}\right)U_i \\
&+ \left(\tfrac{-p_{i-1}}{60h} + \tfrac{7p_i}{15h} + \tfrac{p_{i+1}}{20h} + \tfrac{Q_{i+1}}{30}\right)U_{i+1} - \tfrac{1}{30}\left(g_{i-1} + 28g_i + g_{i+1}\right).
\end{aligned} \quad (30)$$

Now by introducing a constant fitting factor $\sigma(\rho)$ in Eq. (30), we obtain

$$\begin{aligned}
&\left(\sigma(\rho)\varepsilon^2 + \tfrac{p_{i+1}h}{30} - \tfrac{p_{i-1}h}{30}\right)\left(\tfrac{U_{i-1}-2U_i+U_{i+1}}{h^2}\right) \\
&= \left(\tfrac{-p_{i-1}}{20h} + \tfrac{Q_{i-1}}{30} - \tfrac{7p_i}{15h} + \tfrac{p_{i+1}}{60h}\right)U_{i-1} + \left(\tfrac{p_{i-1}}{15h} + \tfrac{14Q_i}{15} - \tfrac{p_{i+1}}{15h}\right)U_i \\
&+ \left(\tfrac{-p_{i-1}}{60h} + \tfrac{7p_i}{15h} + \tfrac{p_{i+1}}{20h} + \tfrac{Q_{i+1}}{30}\right)U_{i+1} - \tfrac{1}{30}\left(g_{i-1} + 28g_i + g_{i+1}\right).
\end{aligned} \quad (31)$$

Multiplying Eq. (31) by h and taking the limit as $h \to 0$, we get

$$\lim_{h\to 0} \sigma(\rho)\varepsilon^2 \left(\frac{U_{i-1} - 2U_i + U_{i+1}}{h}\right) = \frac{p(0)}{2}\left(U_{i+1} - U_{i-1}\right). \quad (32)$$

Now using Eq. (19) in Eq. (32), we get

$$\frac{\sigma(\rho)}{\rho}\left(e^{p(1)\rho}-2+e^{-p(1)\rho}\right)=\frac{p(0)}{2}\left(e^{p(1)\rho}-e^{-p(1)\rho}\right).$$

On simplifying, we get

$$\sigma\left(\rho\right)=\frac{p(0)\rho}{2}\coth\left(\frac{p(1)\rho}{2}\right), \tag{33}$$

which is the required value of the constant fitting factor $\sigma\left(\rho\right)$. Finally, using Eq. (31) and the value of $\sigma\left(\rho\right)$ given by Eq. (33), we obtain the recurrence relationship:

$$E_iU_{i-1}+F_iU_i+G_iU_{i+1}=H_i,\ i=1,2,\cdots,N-1, \tag{34}$$

where,

$$\begin{aligned}
E_i &= -\tfrac{\sigma(\rho)\varepsilon^2}{h^2}-\tfrac{p_{i-1}}{60h}-\tfrac{28p_i}{60h}-\tfrac{p_{i+1}}{60h}+\tfrac{Q_{i-1}}{30},\\
F_i &= \tfrac{2\sigma(\rho)\varepsilon^2}{h^2}+\tfrac{28Q_i}{30},\\
G_i &= -\tfrac{\sigma(\rho)\varepsilon^2}{h^2}+\tfrac{p_{i-1}}{60h}-\tfrac{p_{i+1}}{60h}+\tfrac{28p_i}{60h}+\tfrac{Q_{i+1}}{30},\\
H_i &= \tfrac{1}{30}\left(g_{i-1}+28g_i+g_{i+1}\right).
\end{aligned}$$

The relation (34) represents a system of $(N-1)$ equations with $(N+1)$ unknowns. These $(N-1)$ equations together with the boundary conditions $U(0,t_{j+1})$ and $U(1,t_{j+1})$ given by (11) are sufficient to solve for the unknowns $U(x_1,t_{j+1})$ to $U(x_{N-1},t_{j+1})$.

4. Convergence Analysis

In this section, we prove an ε-uniform convergence of the proposed scheme.

Lemma 4.1. *If $U\in C^3(I)$, then*

$$|\tau_i|\leq\max_{x_{i-1}\leq x\leq x_{i+1}}\left\{\frac{28ph^2}{180}\left|U^{(3)}(x)\right|\right\}+O\left(h^3\right),\ i=1,2,\cdots,N-1. \tag{35}$$

Proof. By definition

$$\begin{aligned}
\tau_i &= -\sigma\varepsilon^2\left\{\tfrac{U_{i-1}-2U_i+U_{i+1}}{h^2}-U_i^{''}\right\}+\tfrac{p_{i-1}}{30}\left\{\left(\tfrac{-3U_{i-1}+4U_i-U_{i-1}}{2h}+hU_i^{''}\right)-U_{i-1}^{'}\right\}\\
&\quad+\tfrac{28p_i}{30}\left\{\tfrac{U_{i+1}-U_{i-1}}{2h}-U_i^{'}\right\}+\tfrac{p_{i+1}}{30}\left\{\left(\tfrac{U_{i+1}-4U_i+3U_{i-1}}{2h}-hU_i^{''}\right)-U_{i+1}^{'}\right\},\\
&\quad i=1(1)N-1,\\
\Rightarrow\tau_i &= -\sigma\varepsilon^2\left\{\tfrac{h^2}{12}U_i^{(4)}+\tfrac{h^4}{360}U_i^{(6)}+\cdots\right\}+\tfrac{p_{i-1}}{30}\left\{hU_i^{''}-\tfrac{2h^2}{3}U_i^{(3)}+\right\}\\
&\quad\text{`}+\tfrac{28p_i}{30}\left\{\tfrac{h^2}{6}U_i^{(3)}+\tfrac{h^4}{120}U_i^{(5)}+\cdots\right\}+\tfrac{p_{i+1}}{30}\left\{-hU_i^{''}-\tfrac{2h^2}{3}U_i^{(3)}+\cdots\right\},\\
\Rightarrow|\tau_i| &\leq\max_{x_{i-1}\leq x\leq x_{i+1}}\left\{\frac{\sigma h^2\varepsilon}{12}\left|U^{(4)}(x)\right|\right\}+\max_{x_{i-1}\leq x\leq x_{i+1}}\left\{\frac{28}{180}ph^2\left|U^{(3)}(x)\right|\right\}.
\end{aligned}$$

Using the relation (34) with $M=\frac{p(0)}{2}\coth\left(\frac{p(1)\rho}{2}\right)$ we get,

$$\Rightarrow |e_i| \leq \max_{x_{i-1}\leq x\leq x_{i+1}} \left\{ \frac{Mh^3}{12} \left| U^{(4)}(x) \right| \right\} + \max_{x_{i-1}\leq x\leq x_{i+1}} \left\{ \frac{28}{180} ph^2 \left| U^{(3)}(x) \right| \right\},$$

$$\Rightarrow |\tau_i| \leq \max_{x_{i-1}\leq x\leq x_{i+1}} \left\{ \frac{28}{180} ph^2 \left| U^{(3)}(x) \right| \right\} + O\left(h^3\right),$$

$$\Rightarrow |\tau_i| \leq C\left(h^2\right),\ i = 1, 2, \cdots, N-1.$$

Thus the desired result is obtained. □

Lemma 4.2. *Let $U(x_i, t_{j+1})$ be the solution of problem (11) and $U_{i,j+1}$ be the solution of the discrete problem (35). Then, we have the following estimate:*

$$|U(x_i, t_{j+1}) - U_{i,j+1}| \leq O\left(h^2\right). \tag{36}$$

Proof. . Rewriting Eq. (34) in matrix vector form as:

$$YU = C, \tag{37}$$

where $Y = (a_{i,j}),\ 1 \leq i, j \leq N-1$ is a tri-diagonal matrix of order $N-1$ with

$$\begin{aligned} a_{i,i-1} &= -\tfrac{\sigma(\rho)\varepsilon^2}{h^2} - \tfrac{p_{i-1}}{60h} - \tfrac{28p_i}{60h} - \tfrac{p_{i+1}}{60h} + \tfrac{Q_{i-1}}{30}, \\ a_{i,i} &= \tfrac{2\sigma(\rho)\varepsilon^2}{h^2} + \tfrac{28Q_i}{30}, \\ a_{i,i+1} &= -\tfrac{\sigma(\rho)\varepsilon^2}{h^2} + \tfrac{p_{i-1}}{60h} - \tfrac{p_{i+1}}{60h} + \tfrac{28p_i}{60h} + \tfrac{Q_{i+1}}{30}, \end{aligned}$$

and $C = H_i$ is a column vector with $H_i = \frac{1}{30}\left(g_{i-1} + 2g_i + g_{i+1}\right)$ for $i = 1, 2, \cdots, N-1$, with local truncation error e_i :

$$|\tau_i| \leq C\left(h^2\right), \tag{38}$$

we also have

$$Y\overline{U} - e(h) = C, \tag{39}$$

where, $\overline{U} = \left(\overline{U}_0, \overline{U}_1, , \cdots, \overline{U}_N\right)^T$ and $e(h) = (e_1(h), e_2(h), , e_2(h), \cdots, e_N(h))^T$ denote the actual solution and the local truncation error respectively.
From Eqs. (37) and (39), we get

$$Y(\overline{U} - U) = \tau(h). \tag{40}$$

Thus, the error equation is

$$YE = \tau(h), \tag{41}$$

where, $E = \overline{U} - U = (e_0, e_1, e_2, \cdots, e_N)^t$. Let S be the sum of elements of the ith row of Y, then we have

$$S_1 = \sum_{j=1}^{N-1} a_{1,j} = \frac{\sigma\varepsilon^2}{h^2} + \frac{p_{i+1}}{60h} + \frac{p_{i-1}}{60h} + \frac{28Q_i}{30} + \frac{Q_{i+1}}{30} + \frac{28p_i}{60h}$$

$$S_{N-1} = \sum_{j=1}^{N-1} a_{N-1,j} = \frac{\sigma\varepsilon^2}{h^2} - \frac{p_{i+1}}{60h} - \frac{p_{i-1}}{60h} + \frac{28Q_i}{30} + \frac{Q_{i-1}}{30} - \frac{28p_i}{60h},$$

$$\begin{aligned} S_i &= \textstyle\sum_{j=1}^{N-1} a_{i,j} = \frac{1}{30}\left(g_{i-1} + 28g_i + g_{i+1}\right), \\ &= s_i + O\left(h^2\right) = B_{i0};\ i = 2\,(1)\,N-2, \end{aligned}$$

where, $B_{i0} = s_i = \frac{1}{30}(g_{i-1} + 28g_i + g_{i+1})$.
Since $0 < \varepsilon << 1$, for sufficiently small h the matrix Y is irreducible and monotone [20]. Then, it follows that Y^{-1} exists and its elements are non-negative. Hence, from Eq. (41), we obtain

$$E = Y^{-1}\tau(h), \tag{42}$$

and

$$\|E\| \leq \left\|Y^{-1}\right\| \|\tau(h)\|. \tag{43}$$

Let $\overline{a}_{ki}$ be the $(ki)\,th$ elements of Y^{-1}. Since $\overline{a}_{ki} \geq 0$ by the definition of multiplication of matrices with its inverses, we have

$$\sum_{i=1}^{N-1} \overline{a}_{ki} S_i = 1,\ k = 1, 2, \cdots, N-1. \tag{44}$$

Therefore, it follows that

$$\sum_{i=1}^{N-1} \overline{a}_{ki} \leq \frac{1}{\min_{0\leq i\leq N-1} S_i} = \frac{1}{B_{i,0}} \leq \frac{1}{|B_{i0}|}, \tag{45}$$

for some $i0$ between 1 and $N-1$, and $B_{i0} = s_i$ From equations (37), (43) and (45), we obtain

$$e_i = \sum_{i=1}^{N-1} \overline{a}_{ki}\tau(h),\ i = 1\,(1)\,N-1,$$

which implies

$$e_i \leq \frac{C\left(h^2\right)}{|s_i|}\ i = 1\,(1)\,N-1. \tag{46}$$

Therefore,

$$\|E\| \leq C\left(h^2\right). \tag{47}$$

This implies that the spatial semi-discretization process is uniformly convergent of second order.

□

Theorem 4.3. *Let $u(x,t)$ be the solution of the problem* (2) *and $U_{i,j+1}$ be the numerical solution obtained by the proposed scheme* (35)*. Then, for sufficiently small h the error estimate for the totally discrete scheme is given by*

$$|u(x_i, t_{j+1}) - U_{i,j+1}| \leq C\left(\Delta t + (h)^2\right). \tag{48}$$

Proof. The triangle inequality gives

$$\begin{aligned}|u(x_i, t_{j+1}) - U_{i,j+1}| &= \max_{i,j} |u(x_i, t_{j+1}) - U(x_i, t_{j+1}) + U(x_i, t_{j+1}) - U_{i,j+1}| \\ &\leq \max_{i,j} |u(x_i, t_{j+1}) - U(x_i, t_{j+1})| + \max_{i,j} |U(x_i, t_{j+1}) - U_{i,j+1}|.\end{aligned}$$

Using Lemma 3.3 and Lemma 4.2, we get the desired result. □

5. Numerical Examples and Results

The applicability and efficiency of the proposed numerical scheme for problem (2) have been checked by considering two model examples. As the exact solutions of these examples are not known, the maximum pointwise error for the given examples are computed by using the double mesh principle [21] defined by:

$$E^{N,M}_{\varepsilon,\delta,\eta} = \max_{1\le i,j\le N-1,M-1} \left| U^{N,M}_{i,j} - U^{2N,2M}_{i,j} \right|,$$

where $U^{N,M}_{i,j}$ are computed numerical solutions obtained on the mesh $D^{N,M} = \Omega^N_x \times \Omega^M_t$ with N mesh intervals in the spatial direction and M mesh intervals in the temporal direction, whereas $U^{2N,2M}_{i,j}$ are computed numerical solutions on the mesh $D^{2N,2M} = \Omega^{2N}_x \times \Omega^{2M}_t$ by adding the midpoint $x_{i+1/2} = (x_{i+1} + x_i)/2$ and $t_{j+1/2} = (t_{j+1} + t_j)/2$ into the mesh points. For any value of N and M , the ε-uniform maximum pointwise errors are calculated using

$$E^{N,M} = \max_{\varepsilon,\delta,\eta} E^{N,M}_{\varepsilon,\delta,\eta}.$$

The rate of convergence of the scheme is calculated by the formula

$$r^{N,M}_{\varepsilon,\delta,\eta} = \frac{\log(E^{N,M}_{\varepsilon,\delta,\eta}) - \log(E^{2N,2M}_{\varepsilon,\delta,\eta})}{\log(2)},$$

and the ε-uniform rate of convergence is calculated by:

$$r^{N,M} = \frac{\log\left(E^{N,M}\right) - \log\left(E^{2N,2M}\right)}{\log(2)}.$$

Example 5.1. In this example, we consider the following singularly perturbed delay parabolic differential equation with interval boundary conditions and the initial condition:

$$\begin{cases} \frac{\partial u(x,t)}{\partial t} - \varepsilon^2 \frac{\partial^2 u(x,t)}{\partial x^2} + (2-x^2)\frac{\partial u(x,t)}{\partial x} + 2u(x-\delta,t) \\ +(x-3)u(x,t) + u(x+\eta,t) = 10t^2\exp(-t)x(1-x), \\ u(x,0) = 0, x \in D_0 = \{(x,0) : x \in \overline{\Omega}_x\}, \\ u(x,t) = 0, \forall (x,t) \in D_L = \{(x,t) : -\delta \le x \le 0, t \in (0,3]\}, \\ u(x,t) = 0, \forall (x,t) \in D_R = \{(x,t) : 1 \le x \le 1+\eta, t \in (0,3]\}. \end{cases}$$

Example 5.2. Now, we consider the following singularly perturbed delay parabolic differential equation with interval boundary conditions and the initial condition:

$$\begin{cases} \frac{\partial u(x,t)}{\partial t} - \varepsilon^2 \frac{\partial^2 u(x,t)}{\partial x^2} + \left(2-x^2\right)\frac{\partial u(x,t)}{\partial x} + (1+x)u(x-\delta,t) + \\ (x^2+1+\cos(\pi x))u(x,t) + 3u(x+\eta,t) = \sin(\pi x), \\ u(x,0) = 0, x \in D_0 = \{(x,0) : x \in \overline{\Omega}_x\}, \\ \phi(x,t) = 0, \forall (x,t) \in D_L = \{(x,t) : -\delta \le x \le 0, t \in (0,3]\}, \\ \psi(x,t) = 0, \forall (x,t) \in D_R = \{(x,t) : 1 \le x \le 1+\eta, t \in (0,3]\}. \end{cases}$$

The $E^{N,M}_{\varepsilon,\delta,\eta}$, $r^{N,M}_{\varepsilon,\delta,\eta}$, $E^{N,M}$ and $r^{N,M}$ for Example 5.1 obtained by the proposed method and comparison with results in [12] are presented in Table 1 for various values of ε and N. Besides, a comparison of numerical results of Example 5.1

TABLE 1. Example 5.1 $E^{N,M}_{\varepsilon,\delta,\eta}, r^{N,M}_{\varepsilon,\delta,\eta}, E^{N,M}$ and $r^{N,M}$ for the proposed method and results in [12] with $T = 1.0, \delta = 0.5 \times \varepsilon, M = N$

$\varepsilon \downarrow$	N=32	N=64	N=128	N=256	N=512	1024
	Our Result					
10^0	1.6354e-04	8.3357e-05	4.2110e-05	2.1180e-05	1.0621e-05	5.3186e-06
10^{-1}	2.6447e-03	8.5157e-04	3.9013e-04	2.1208e-04	1.1070e-04	5.6559e-05
10^{-2}	3.6361e-03	2.1975e-03	1.2043e-03	6.2974e-04	3.2190e-04	1.6168e-04
10^{-3}	3.6277e-03	2.1901e-03	1.2002e-03	6.2754e-04	3.2078e-04	1.6216e-04
10^{-4}	3.6268e-03	2.1894e-03	1.1998e-03	6.2732e-04	3.2067e-04	1.6210e-04
10^{-5}	3.6268e-03	2.1894e-03	1.1998e-03	6.2732e-04	3.2067e-04	1.6210e-04
10^{-6}	3.6268e-03	2.1894e-03	1.1998e-03	6.2732e-04	3.2067e-04	1.6210e-04
10^{-8}	3.6268e-03	2.1894e-03	1.1998e-03	6.2732e-04	3.2067e-04	1.6210e-04
$E^{N,M}$	3.6361e-03	2.1975e-03	1.2043e-03	6.2974e-04	3.2190e-04	1.6168e-04
$r^{N,M}$	7.2653e-01	8.6767e-01	9.3537e-01	9.6814e-01	9.9347e-01	
	Results in [12]					
10^0	1.49e-03	7.21e-04	3.56e-04	1.77e-04	8.83e-05	4.41e-05
10^{-1}	3.71e-03	1.90e-03	1.03e-03	5.29e-4	2.66e-04	1.34e-04
10^{-2}	5.20e-03	3.02e-03	1.67e-03	9.10e-04	4.93e-04	2.66e04
10^{-3}	4.70e-03	2.84e-03	1.68e-03	9.56e-04	5.31e-04	2.88e-04
10^{-4}	4.71e-03	2.74e-03	1.60e-03	9.05e-04	5.05e-04	2.79e-04
10^{-5}	4.71e-03	2.72e-03	1.59e-03	8.95e-04	4.95e-04	2.71e-04
10^{-6}	4.71e-03	2.72e-03	1.59e-03	8.95e-04	4.95e-04	2.71e-04
10^{-8}	4.71e-03	2.72e-03	1.59e-03	8.95e-04	4.95e-04	2.71e-04
$E^{N,M}$	5.20e-03	3.02e-03	1.68e-03	9.56e-04	5.31e-04	2.88e-04
$r^{N,M}$	.78	.85	.81	.85	.88	

obtained by the proposed method and results in [9] is tabulated in Table 2. It can be concluded from Tables 1 and 2 that the proposed method provides more accurate solutions than recent results in [12] and [9].

TABLE 2. Example 5.1: $E^{N,M}_{\varepsilon,\delta,\eta}, E^{N,M}$ and $r^{N,M}$ for the proposed method and results in [9] with $T = 3.0, \delta = 0.5 \times \varepsilon, M = N$

ε $\downarrow$	M=60 N=32	M=120 N=64	M=240 N=128	M=480 N=256	M=960 N=512	1920 1024
	Our Result					
2^{-6}	5.7119e-03	3.0954e-03	1.6719e-03	8.7253e-04	4.3743e-04	1.8654e-04
2^{-8}	5.6564e-03	3.0651e-03	1.6551e-03	8.6397e-04	4.4129e-04	2.2300e-04
2^{-10}	5.6427e-03	3.0576e-03	1.6510e-03	8.6180e-04	4.4019e-04	2.2244e-04
2^{-12}	5.6393e-03	3.0557e-03	1.6500e-03	8.6126e-04	4.3991e-04	2.2230e-04
2^{-14}	5.6384e-03	3.0552e-03	1.6497e-03	8.6112e-04	4.3984e-04	2.2227e-04
2^{-16}	5.6382e-03	3.0551e-03	1.6496e-03	8.6109e-04	4.3982e-04	2.2226e-04
2^{-18}	5.6382e-03	3.0551e-03	1.6496e-03	8.6109e-04	4.3982e-04	2.2226e-04
2^{-20}	5.6382e-03	3.0551e-03	1.6496e-03	8.6109e-04	4.3982e-04	2.2226e-04
$E^{N,M}$	5.7119e-03	3.0954e-03	1.6719e-03	8.7253e-04	4.4129e-04	2.2300e-04
$r^{N,M}$	8.8384e-01	8.8864e-01	9.3821e-01	9.8348e-01	9.8468e-01	
	Results in [9]					
2^{-6}	7.3811e-03	4.3778e-03	2.1211e-03	1.0929e-03	5.5057e-04	2.7589e-04
2^{-8}	7.4985e-03	4.4456e-03	2.3806e-03	1.2446e-03	5.7770e-04	2.7788e-04
2^{-10}	7.5020e-03	4.4954e-03	2.4363e-03	1.2530e-03	6.2975e-04	3.2015e-04
2^{-12}	7.4982e-03	4.4966e-03	2.4448e-03	1.2716e-03	6.4618e-04	3.2225e-04
2^{-14}	7.4970e-03	4.4961e-03	2.4450e-03	1.2728e-03	6.4893e-04	3.2545e-04
2^{-16}	7.4966e-03	4.4959e-03	2.4450e-03	1.2728e-03	6.4909e-04	3.2774e-04
2^{-18}	7.4966e-03	4.4958e-03	2.4449e-03	1.2728e-03	6.4909e-04	3.2774e-04
2^{-20}	7.4965e-03	4.4958e-03	2.4449e-03	1.2728e-03	6.4909e-04	3.2774e-04
$E^{N,M}$	7.5020e-03	4.4966e-03	2.4450e-03	1.2728e-03	6.4909e-04	3.2774e-04
$r^{N,M}$	0.7384	0.8791	0.9418	0.9715	0.9859	

Table 3 shows a computed $E^{N.M}_{\varepsilon,\delta,\eta}, r^{N.M}_{\varepsilon,\delta,\eta}, E^{N.M}$ and $r^{N.M}$ for Example 5.2 with $\delta = \eta = 0.5\times\varepsilon$ and for different values of ε and N. Moreover, a comparison of the computed numerical results by the proposed method for $T = 3, \delta = 0.6 \times \varepsilon, \eta = 0.5 \times \varepsilon$ and different values of ε and N is presented in Table 4 with the results in [9]. From this table, one can observe that the proposed scheme gives more accurate results than results in [9].

TABLE 3. Example 5.2: $E^{N,M}_{\varepsilon,\delta,\eta}, r^{N,M}_{\varepsilon,\delta,\eta}, E^{N,M}$ and $r^{N,M}$ for the proposed method with $T = 3.0, \delta = \eta = 0.5 \times \varepsilon, M = N$

$\varepsilon \downarrow$	N=32	N=64	N=128	N=256	N=512	1024
10^{0}	4.5117e-03	2.8946e-03	1.7893e-03	9.9653e-04	5.3027e-04	2.7393e-04
	6.4031e-01	6.9397e-01	8.4441e-01	9.1019e-01	9.5292e-01	
10^{-1}	7.9508e-03	4.8116e-03	2.7152e-03	1.4522e-03	7.5168e-04	3.8219e-04
	7.2458e-01	8.2546e-01	9.0282e-01	9.5005e-01	9.7583e-01	
10^{-2}	8.0520e-03	5.0091e-03	2.8755e-03	1.5525e-03	8.0567e-04	4.1008e-04
	6.8480e-01	8.0074e-01	8.8922e-01	9.4633e-01	9.7428e-01	
10^{-3}	8.0491e-03	5.0051e-03	2.8716e-03	1.5497e-03	8.0408e-04	4.0925e-04
	6.8543e-01	8.0154e-01	8.8987e-01	9.4658e-01	9.7143e-01	
10^{-4}	8.0488e-03	5.0047e-03	2.8712e-03	1.5494e-03	8.0392e-04	4.0917e-04
	6.8554e-01	8.0163e-01	8.8994e-01	9.4659e-01	9.7435e-01	
10^{-5}	8.0488e-03	5.0046e-03	2.8712e-03	1.5494e-03	8.0390e-04	4.0916e-04
	6.8552e-01	8.0160e-01	8.8994e-01	9.4662e-01	9.7435e-01	
10^{-6}	8.0488e-03	5.0046e-03	2.8712e-03	1.5494e-03	8.0390e-04	4.0916e-04
	6.8552e-01	8.0160e-01	8.8994e-01	9.4662e-01	9.7435e-01	
10^{-8}	8.0488e-03	5.0046e-03	2.8712e-03	1.5494e-03	8.0390e-04	4.0916e-04
	6.8552e-01	8.0160e-01	8.8994e-01	9.4662e-01	9.7435e-01	
$E^{N,M}$	8.0520e-03	5.0091e-03	2.8755e-03	1.5525e-03	8.0567e-04	4.1008e-04
$r^{N,M}$	6.8480e-01	8.0074e-01	8.8922e-01	9.4633e-01	9.7428e-01	

TABLE 4. Example 5.2: $E^{N,M}_{\varepsilon,\delta,\eta}, r^{N,M}_{\varepsilon,\delta,\eta}, E^{N,M}$ and $r^{N,M}$ for the proposed method and results in [9] with $T = 3.0, \delta = 0.6\times\varepsilon, \eta = 0.5 \times \varepsilon, M = N$

ε $\downarrow$	M=30 N=16	M=60 N=32	M=120 N=64	M=240 N=128	M=480 N=256	M=960 N=512
	Our Result					
2^{-6}	7.7532e-03	4.6663e-03	2.6329e-03	1.4068e-03	7.2606e-04	3.6799e-04
2^{-8}	7.7495e-03	4.6613e-03	2.6279e-03	1.4033e-03	7.2404e-04	3.6736e-04
2^{-10}	7.7485e-03	4.6601e-03	2.6266e-03	1.4024e-03	7.2353e-04	3.6709e-04
2^{-12}	7.7482e-03	4.6597e-03	2.6263e-03	1.4022e-03	7.2341e-04	3.6703e-04
2^{-14}	7.7482e-03	4.6597e-03	2.6262e-03	1.4021e-03	7.2337e-04	3.6701e-04
2^{-16}	7.7482e-03	4.6596e-03	2.6262e-03	1.4021e-03	7.2337e-04	3.6701e-04
2^{-18}	7.7482e-03	4.6596e-03	2.6262e-03	1.4021e-03	7.2337e-04	3.6701e-04
2^{-20}	7.7482e-03	4.6596e-03	2.6262e-03	1.4021e-03	7.2337e-04	3.6701e-04
$E^{N,M}$	7.7532e-03	4.6663e-03	2.6329e-03	1.4068e-03	7.2606e-04	3.6799e-04
$r^{N,M}$	7.3251e-01	8.2563e-01	9.0424e-01	9.5426e-01	9.8042e-01	

ε $\downarrow$	M=30 N=16	M=60 N=32	M=120 N=64	M=240 N=128	M=480 N=256	M=960 N=512
	Results in [9]					
2^{-6}	1.5094e-02	7.5604e-03	3.8074e-03	1.9127e-03	9.5839e-04	4.7957e-04
2^{-8}	1.5222e-02	7.6300e-03	3.8341e-03	1.9259e-03	9.6541e-04	4.8335e-04
2^{-10}	1.5237e-02	7.6373e-03	3.8377e-03	1.9274e-03	9.6613e-04	4.8372e-04
2^{-12}	1.5240e-02	7.6385e-03	3.8382e-03	1.9277e-03	9.6624e-04	4.8378e-04
2^{-14}	1.5240e-02	7.6387e-03	3.8383e-03	1.9277e-03	9.6627e-04	4.8378e-04
2^{-16}	1.5241e-02	7.6388e-03	3.8384e-03	1.9277e-03	9.6627e-04	4.8379e-04
2^{-18}	1.5241e-02	7.6388e-03	3.8384e-03	1.9277e-03	9.6627e-04	4.8379e-04
2^{-20}	1.5241e-02	7.6388e-03	3.8384e-03	1.9277e-03	9.6627e-04	4.8379e-04
$E^{N,M}$	1.5241e-02	7.6388e-03	3.8384e-03	1.9277e-03	9.6627e-04	4.8379e-04
$r^{N,M}$	0.9924	0.9925	0.9925	0.9964	0.9981	

The graphical representations of the computed numerical solutions for Examples 5.1 and 5.2 at different values of time t and by taking $\varepsilon = 2^{-3}, N = 100, M = 120$ are shown in Figures 1(A) and (B) respectively.

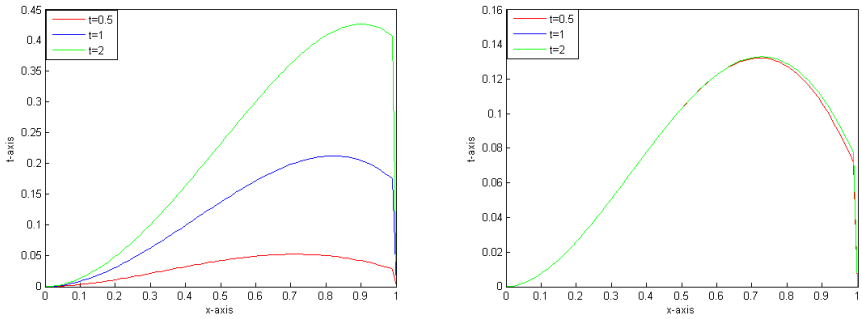

(A) Example 5.1 (B) Example 5.2

FIGURE 1. The numerical solution profiles for $T = 3.0, \varepsilon = 2^{-3}, \delta = 0.6 \times \varepsilon, \eta = 0.5 \times \varepsilon, N = 100, M = 120$ and at different time step size t.

To show the effect of singular perturbation parameter and shifts on the boundary layer behaviour of the solutions, we solved the considered test examples for the varying values of ε, δ and η and have plotted the graphs of the solution in Figures 2-4. Figures 2(A) and (B)represent the graphs of the solution for various values of ε with fixed $\delta = 0.6\times$ and $\eta = 0.5 \times \varepsilon$.

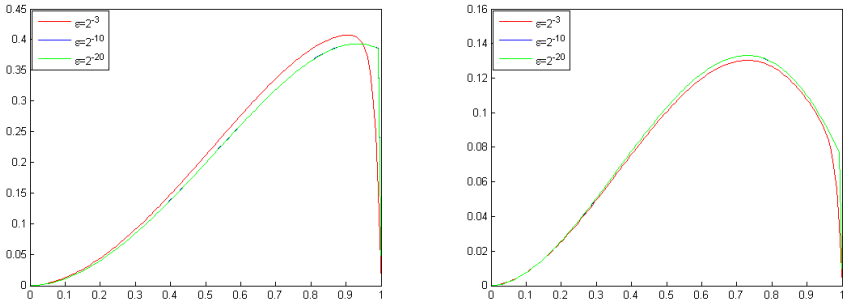

(A) Example 5.1 (B) Example 5.2

FIGURE 2. Effect of ε on the solution behavior at $T = 3,$, $\delta = 0.6 \times \varepsilon$ and $\eta = 0.5 \times \varepsilon$

Figures 3(A) and (B)represent the graphs of the solution for different values of δ with fixed $\varepsilon = 2^{-3}$ and $\eta = 0.5 \times \varepsilon$, whereas Figures 4(A) and (B)represent the graphs of the solution for various values of η with fixed $\varepsilon = 2^{-3}$ and $\delta = 0.6 \times \varepsilon$. It

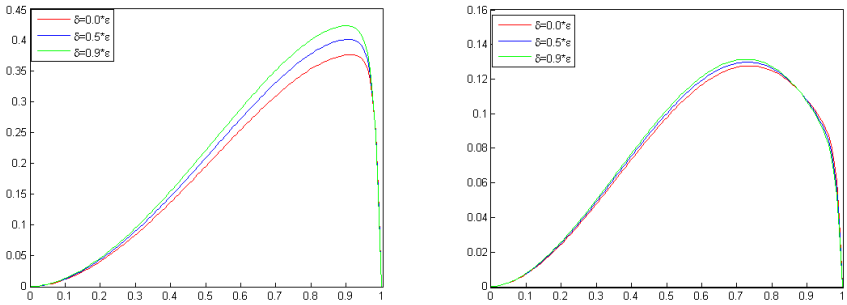

(A) Example 5.1 (B) Example 5.2

FIGURE 3. Effect of δ on the solution behavior at $\varepsilon = 2^{-3}, \eta = 0.5 \times \varepsilon, N = M = 128$.

has been observed from Figures 4 (A) and (B), when the perturbation parameter tends to zero strong boundary layer is formed at the right endpoints of the underlying interval.

As the size of the delay parameter increases, the thickness of the layer increases (see 3(A) and (B)). On the other hand, if the size of the advance parameter increases, the thickness of the layer decreases (see 4(A) and (B)).

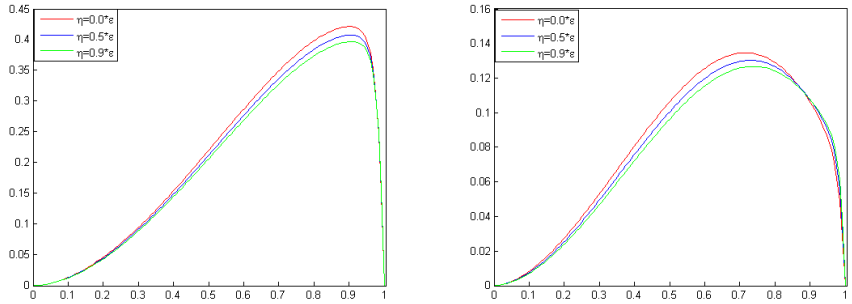

(A) Example 5.1 (B) Example 5.2

FIGURE 4. Effect of η on the solution behavior at $\varepsilon = 2^{-3}, \delta = 0.6 \times \varepsilon, N = M = 128$.

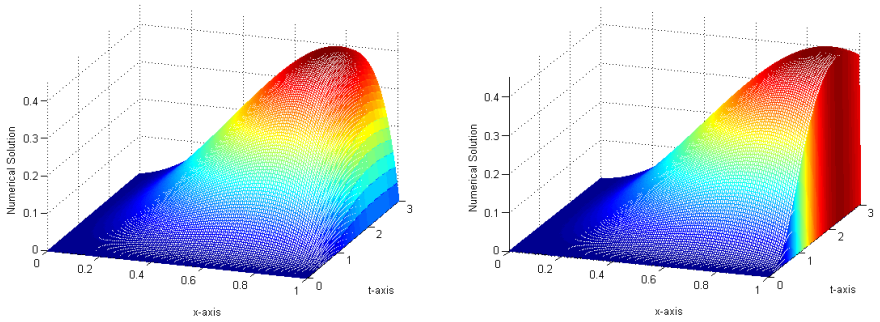

(A) $\varepsilon = 2^{-2}$ (B) $\varepsilon = 2^{-20}$

FIGURE 5. Numerical solution profiles for Example 5.1 for $T = 3.0, \delta = 0.6 \times \varepsilon, \eta = 0.5 \times \varepsilon, N = M = 128$.

Figure 5(A) and (B) depict the numerical solution profiles for Example 5.1 at (A) $\varepsilon = 2^{-2}, T = 3, \delta = 0.6 \times \varepsilon, \eta = 0.5 \times \varepsilon, N = M = 128$ and (B) $\varepsilon = 2^{-20}, T = 3, \delta = 0.6 \times \varepsilon, \eta = 0.5 \times \varepsilon, N = M = 128$ respectively.

The numerical solution profiles for Example (5.2) is displayed in Figure (6) (A) and (B) at (A) $\varepsilon = 2^{-2}, T = 3, \delta = 0.6 \times \varepsilon, \eta = 0.5 \times \varepsilon, N = 128$ and (B) $\varepsilon = 2^{-20}, T = 3, \delta = 0.6 \times \varepsilon, \eta = 0.5 \times \varepsilon, N = 128$ respectively. From Tables 1-4 , we observe that the numerical results obtained by the proposed method is in agreement with the theoretical results stated in Theorem 4.3. It is pertinent to claim that the proposed method provides $\varepsilon-$uniform, more accurate and improves the numerical results as compared to some existing methods

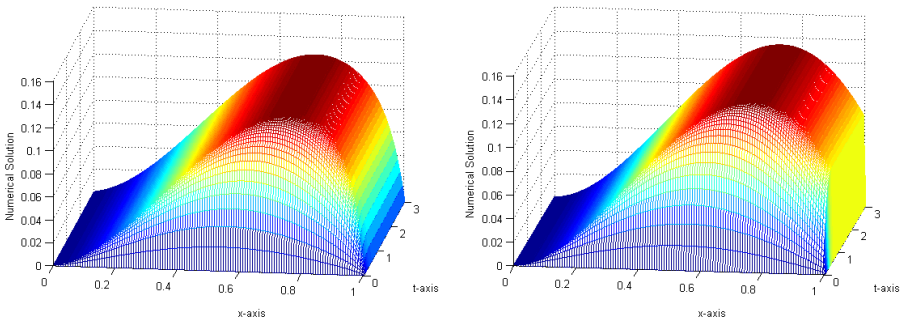

(A) $\varepsilon = 2^{-2}$ (B) $\varepsilon = 2^{-20}$

FIGURE 6. Numerical solution profiles for Example 5.1 for $T = 3.0, \delta = 0.6 \times \varepsilon, \eta = 0.5 \times \varepsilon, N = M = 128$.

6. Conclusions

An exponentially fitted numerical scheme has been proposed for solving SPDP-PDEs with small mixed shifts in the reaction terms and spatial variable arising in computational neuroscience whose solution exhibits a boundary layer located at x = 1. The scheme has shown to be $\varepsilon-$uniformly convergent of first-order in the time direction and second-order in the space direction.The efficiency of the proposed scheme has been shown by taking two model examples and comparing them with the numerical results in [9] and [12]. It has been observed that the proposed numerical scheme provides more accurate numerical results than numerical schemes in [9] and [12]. One can observe from Tables 1-4 that $E_{\varepsilon,\delta}^{N,M}$ decreases as $\varepsilon \to 0$ and mesh size decreases, which indicates that the scheme is $\varepsilon-$ uniformly convergent and stable.

ACKNOWLEDGEMENTS: The authors would like to thank the anonymous referees for their helpful comments that improved the quality of this paper.

CONFLICT OF INTEREST: The authors declared no potential conflicts of interest with respect to the research, authorship and publication of this article.

REFERENCES

1. R.B. Stein, *Some models of neuronal variability*, Biophysical journal **7** (1967), 37-68.
2. M.W. Derstine, H.M. Gibbs, F.A. Hopf and D.L. Kaplan, *Bifurcation gap in a hybrid optically bistable system*, Phys. Rev. A **26** (1982), 3720-3722.
3. M. Wazewska-Czyzewska and A. Lasota, *Mathematical models of the red cell system*, Mat. Stos. **6** (1976), 25-40.
4. A. Longtin and J.G. Milton, *Complex oscillations in the human pipil light reflex with mixed and delayed feedback*, Math. Biosci. **90** (1988), 183-189.

5. V.Y. Glizer, *Asymptotic solution of a boundary-value problem for linear singularly perturbed functional differential equations arising in optimal control theory*, J. Optim. Theory Appl. **106** (2000), 309-335.
6. V. Gupta, M. Kumar and S. Kumar, *Higher order numerical approximation for time dependent singularly perturbed differential-difference convection-diffusion equations*, Numer. Methods Partial Differential Eq. **34** (2018), 357-380.
7. M. Musila and P. Lansky, *Generalized Stein's model for anatomically complex neurons*, BioSystems **25** (1991), 179-191.
8. V.P. Ramesh and M.K. Kadalbajoo, *Upwind and midpoint difference methods for time dependent differential difference equations with layer behavior*, Applied Mathematics and Computational **202** (2008), 453-471.
9. D. Kumar and M.K. Kadalbajoo, *A parameter-uniform numerical method for time-dependent singularly perturbed differential-difference equations*, Applied Mathematical Modelling **35** (2011), 2805-2819.
10. K. Bansal, P. Rai and K.K. Sharma, *Numerical treatment for the class of time dependent singularly perturbed parabolic problems with general shift arguments*, Differ. Equ. Dyn. Syst. **25** (2017), 326-346.
11. K. Bansal and K.K. Sharma, *Parameter uniform numerical scheme for time dependent singularly perturbed convection-diffusion-reaction problems with general shift arguments*, Numer. Algor. **75** (2017), 113-145.
12. D. Kumar, *An implicit scheme for singularly perturbed parabolic problem with retarded terms arising in computational neuroscience*, Numerical Methods for Partial Differential Equations **34** (2018), 1933-1952.
13. V.P. Ramesh and B. Priyanga, *Higher order uniformly convergent numerical algorithm for time-dependent singularly perturbed differential-difference equations*, Differ. Equ. Dyn. Syst. **29** (2021), 239-263.
14. M.M. Woldaregay and G.F. Duressa, *Parameter uniform numerical method for singularly perturbed parabolic differential difference equations*, Journal of the Nigerian Mathematical Society **38** (2019), 223-245.
15. I.T. Daba and G.F. Duressa, *Extended cubic B-spline collocation method for singularly perturbed parabolic differential-difference equation arising in computational neuroscience*, International Journal for Numerical Methods in Biomedical Engineering **37** (2020), e3418.
16. V.A. Solonnikov, O.A. Ladyzenskaja, and N.N. Uralceva, *Linear and quasi linear equations of parabolic type*, American Mathematical Society Providence, Rhode Island, 1988.
17. R.E. O'Malley, *Introduction to singular perturbations*, North-Holland Series in Applied Mathematics & Mechanics, Academic Press Inc., New York, 1974.
18. R.B. Kellogg and A. Tsan, *Analysis of some difference approximations for a singular perturbation problem without turning points*, Math. Comput. **32** (1978), 1025-1039.
19. H. Tian, *The exponential asymptotic stability of singularly perturbed delay differential equations with a bounded layer*, Journal of Mathematical Analysis and Applications **270** (2002), 143-149.
20. R. Ranjan and H.S. Prasad, *A novel approach for the numerical approximation to the solution of singularly perturbed differential-difference equations with small shifts*, Journal of Applied Mathematics and Computing **65** (2021), 403-427.
21. E.P. Doolan, J.J.H. Miller and W.H.A. Schilders , *Uniform numerical methods for problems with initial and boundary layers*, Doole Press, Dublin, 1980.

Imiru Takele Daba received M.Sc. from Haramaya University, Ethiopia and Ph.D. student at Wollega University, Ethiopia. His research interests include Numerical Methods for Singularly Perturbed Differential Equations.

Department of Mathematics, College of Natural Sciences, Wollega University, Nekemte, Oromia, P.O.Box 395, Ethiopia.

e-mail: imirutakele@gmail.com

Gemechis File Duressa received his M.Sc. degree from Addis Ababa University, Ethiopia and Ph.D. degree from National Institute of Technology, Warangal, India. He is currently working as an Associate professor of Mathematics at Jimma University. His research interests include Numerical Methods for Singularly Perturbed Differential Equations(both ODE and PDE). So far he has published more than 80 research articles in reputable journals.

Department of Mathematics, College of Natural Sciences, Jimma University, Jimma, Oromia, P.O.Box 378, Ethiopia.
e-mail: gammeef@gmail.com